ONSET OF DECONFINEMENT AND SEARCH FOR CRITICAL POINT BY NA49 AND NA61 AT CERN SPS

G.L.Melkumov[1] (for the NA49 and NA61 Collaborations)

JINR, 141980, Dubna, Moscow region, Russia

Abstract

The NA49 results on hadron production obtained in Pb+Pb collisions at CERN SPS energies from 20*A* GeV to 158*A* GeV are shown and discussed as evidence for the onset of deconfinement. The signatures of the onset of deconfinement, found by the NA49 experiment at low SPS energies, are confronted with new results from the Beam Energy Scan program at BNL RHIC and CERN LHC results.

A possible indication of the QCD critical point signatures was investigated in the event-by-event fluctuations of various observables such as the mean transverse momentum, particle multiplicity and azimuthal angle as well as the chemical (particle ratio) fluctuations, intermittency of di-pions and net-protons are presented.

A primary conception and plans for continuation of this research program at the SPS by experiment NA61 are briefly discussed.

1 Introduction

It was early shown [1] that nucleus-nucleus collisions at the CERN SPS offered the possibility of reaching energy densities in excess of about 1 GeV/fm^3 during the early stage of the reaction. Under these conditions QCD predicts a phase transition between hadronic matter and state of quasifree quarks and gluons called the quark- gluon plasma (QGP).

Indeed, the predicted signatures of the QGP, e.g. strangeness enhancement, charmonia suppression and dilepton enhancement were observed in Pb+Pb collisions at the top SPS energy ($\sqrt{s_{NN}}$ = 17.3 GeV). Following these observations of a new state of matter [2], the energy dependence of inclusive hadronic observables, i.e. the K/π ratio, the total pion yield and the slope parameter of hadron transverse momentum spectra gave evidence that the predicted signatures of the onset of deconfinement transition [3] is observed at low SPS energies around $\sqrt{s_{NN}} = 8$ GeV [4, 5, 6, 7]. Final results from these studies will be reviewed.

Further insight into the early stage of nucleus-nucleus collisions was motivated by predictions from modern lattice QCD and the QCD model calculations indicating the primaty features of the phase diagram of strongly interacting matter (Fig.1). The QCD suggests that deconfined matter (QGP) is separated from hadron phase, hadron gas (HG), by a first order transition boundary at large bariochemical potential μ_B ending in a critical point E and then turning into a cross-over transition at low values of μ_B (low baryon density). A recent extension to the finite μ_B domain allowed to estimate the position of the critical point E [8].

The location of the hadron chemical freeze-out points of the high density fireball produced in nucleus-nucleus collisions shown in Fig.1. They are obtained from fits of a statistical hadron gas model to hadron abundandances [9, 10, 11]. It provides a good fit to the total yields of numerous particle species with 3 parametrs, namely a temperature T, a baryochemical potential μ_B and a strangeness saturation parameter γ_s. The resulting freeze-out points for central Pb+Pb collisions in the CERN SPS energy range are seen to approach the estimated phase boundary and the critical point E.

[1]E-mail: Georgui.Melkoumov@cern.ch

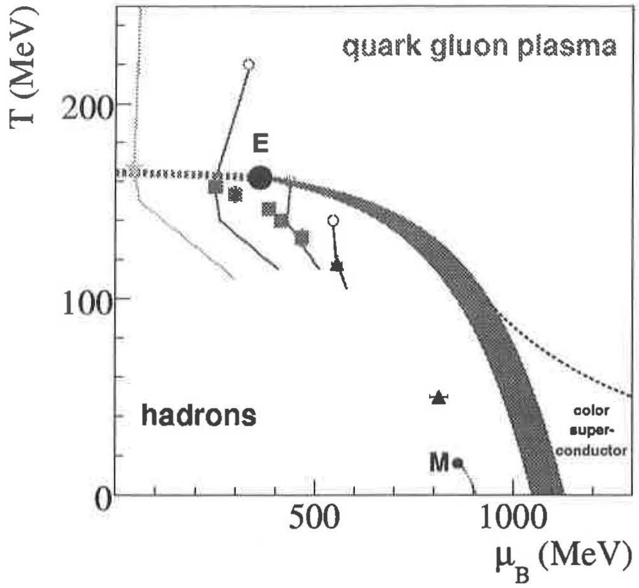

Figure 1: Phase diagram of strongly interacting matter in the plane temperature (T) versus barionic chemical potential (μ_B). The dark band is a lattice QCD estimate [8] of the first order phase boundary between quark-gluon plasma (OGP) and hadrons which ends in a critical point E and then proceeds to a crossover. Symbols denote the chemical freeze-out parameters of heavy ion collisions at different energies as extracted by statistical model fits [9, 10, 11] to the data of the hadron composition at RHIC (STAR), SPS (NA49), AGS and SIS. The open symbols schematically indicate possible values of initial parameters of the reaction systems, which then might evolve along paths as depicted by the vertical lines.

In the vicinity of the QCD critical point a large event-by-event fluctuations of various observables are expected [12, 13]. This paper reports the status of the search for such fluctuations. Results will be presented from analysis of central Pb+Pb collisions, which were recorded for SPS beam energies of 20A, 30A, 40A, 80A and 158A GeV ($\sqrt{s_{NN}}$ = 6.3, 7.6, 8.7, 12.3 and 17.3 GeV) as well as from p+p, C+C and Si+Si interactions at 158A GeV.

The experiment was carried out with the NA49 large acceptance hadron detector [14] employing a system of time projection chambers (TPCs) for efficient tracking in the forward hemisphere of the reactions, precise momentum reconstruction in the magnetic field with a resolution of $\sigma(p)/p^2 \cong (0.3 - 7) \cdot 10^{-4}$ (GeV/c)$^{-1}$ and particle identification using the energy loss dE/dx in the TPC gas. Two time of flight (TOF) walls of 900 scintillator pixels each situated symmetrically to the beam line behined TPCs augment particle identification near midrapidity. The typical dE/dx resolution was $\sigma(dE/dx)/\langle dE/dx\rangle \approx 0.04$ and for TOF resolution $\sigma(TOF) \approx 60$ ps.

2 Onset of deconfinement in hadron production

There is a firm notion that in central collisions of heavy nuclei at the top SPS energy ($\sqrt{s_{NN}}$ = 17.3 GeV) as well as at RHIC energies ($\sqrt{s_{NN}}$ = 130 and 200 GeV) a transient state of deconfined quarks and gluons (QGP) is produced. It is argued by the observation of the signatures predicted for the QGP.

In order to find out whether the early stage fireball actually reaches hadron deconfinement the energy dependence of the hadron production properties was studied [4]. This program was originally motivated by the predictions of the Statistical Model of the Early Stage (SMES) [3]

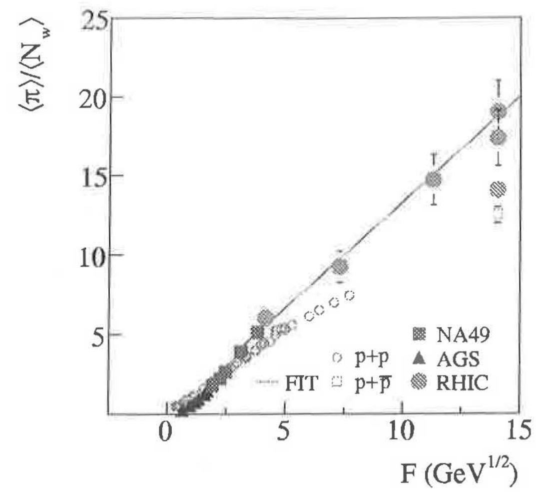

Figure 2: Total pion yield in a full phase space (4π) per wounded nucleons as a function of the Fermi variable $F = (\sqrt{s_{NN}} - 2m_N)^{3/4}/\sqrt{s_{NN}^{1/2}} \approx \sqrt{s_{NN}^{1/2}}$.

assuming that the energy threshold for deconfinement is located at low SPS energies. Several structures in excitation functions were expected within the SMES: a kink in the increase of the pion yield per participant nucleon (change of slope due to increased entropy as a consequence of the activation of partonic degrees of freedom), a sharp peak (horn) in the strangeness to entropy ratio, and a step in the inverse slope parameter of transverse mass spectra (constant temperature and pressure in a mixed phase). Such signatures were indeed observed in $A + A$ collisions by the NA49 experiment [14], thus locating the onset of deconfinement (OD) energy around $30A$ GeV ($\sqrt{s_{NN}} \approx 7.6$ GeV).

2.1 Charged pion yields

Fig.2 shows the pion yield in full phase space of central Pb+Pb collisions [4], normalized to the number of wounded nucleons N_w as a function of the collision energy expressed in a Fermi variable $F \approx \sqrt{s_{NN}^{1/2}}$.

The pions are the most abundantly produced particle species, therefore they measure the early stage entropy density created in the system as it stated in a statistical model approach. Compared to the same data in p+p interaction one can see that the energy dependence of the pion yield in A+A collisions changes its behaviour in the SPS energy region. It clearly steepens at low energies around $30A$ GeV and can be interpreted as an increase of the number of effective degrees of freedom by a factor ≈ 3 [3]. Such an increase may be considered as a consequence of the activation of partonic degrees of freedom when going from hadron gas to QGP.

2.2 Strangeness to pion ratio

Another remarkable observation is a pronounced sharp maximum of K^+/π^+ ratio in central Pb+Pb collisions at about $30A$ GeV beam energy [4] presented in Fig.3 (left). This feature is not seen in p+p interactions and not reproduced by the hadron-string models RQMD [15] , UrQMD [16] or HSD [17].

Since K^+ is by far the most abundant carrier of anti-strangeness at SPS energies, it provides a good measure of the total strangeness produced in the collisions. Thus, the K^+/π^+ ratio represents the strangeness to entropy ratio. A sharp maximum in this quantity was predicted by the SMES consideration as a consequence of the transition to a deconfined

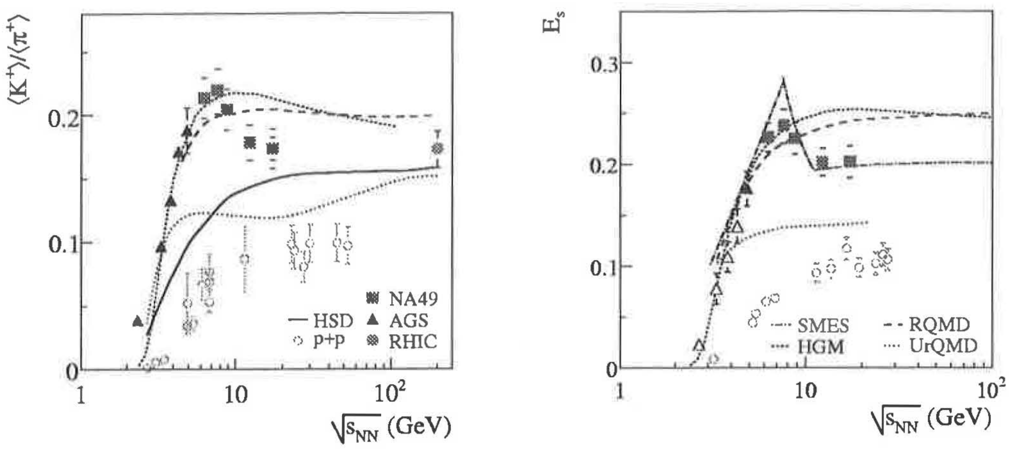

Figure 3: Energy dependence of the $\langle K^+\rangle/\langle\pi^+\rangle$ ratio in full phase space (left). Ratio $E_S = (\langle K + \bar{K}\rangle + \langle\Lambda\rangle)/\langle\pi\rangle$ of total number of strangeness carriers to entropy (pions) versus collision energy (right). NA49 results in Pb+Pb collisions are shown together with the data in A+A collisions at lower and higher energies, and compared to the measurements in p+p reactions. Curves show model predictions.

state [3]. The most relevant measure of the strangeness to entropy ratio used in this work is E_S calculated from π, K and Λ total yields in 4π acceptance. The energy dependence of E_S in central Pb+Pb collisions is plotted in Fig.3 (right).

2.3 Kaon transverse mass distributions

A phase transition was expected to also exhibit itself in the momentum distributions. Fig.4 shows the inverse slope parameters for K^+ and K^- [4] derived from transverse mass spectra of these particles at midrapidity as a function of the collision energy. One observes for slope parameter in A+A collisions a steep rise at lower AGS energies turning into plateau over the entire SPS energy range and then gradually increasing towards RHIC energies. This structure is not seen in p+p reactions and not reproduced by transport models UrQMD [16] and HSD [17].

Since the slope parameter measures both the local temperature and the pressure induced collective flow the step-like behavour observed for the kaon slopes is consistent with the constant temperature and pressure, the features pecular for the mixed phase of a first-order phase transition. Indeed, a hydrodynamical model [18] incorporating a deconfimenent phase transition provides a satisfying description of the experimental data. The step-like behaviour was shown [4] to be a characteristic feature also for pions, protons and antiprotons.

Above feature attributed to the softest point of the equation of state as expected in the first order phase transition is also seen in the excitation function of sound velocity c_s [19], which has been derived from the width of the pion rapidity distributions of the NA49 using the Landau hydrodynamical model.

Finally, in conjuction with the transverse mass spectra, the fireball volume derived from the Bose-Einstein correlations allowed to extract the energy dependence the pion phase space density [20]. This quantity exhibits a plateau at SPS energies, which may also be related to the onset of deconfinement.

The NA49 data on hadron production at SPS energies have recently been confirmed by preliminary data from the STAR experiment at $\sqrt{s_{NN}} = 9.3$ and 19.6 GeV [21, 22, 23].

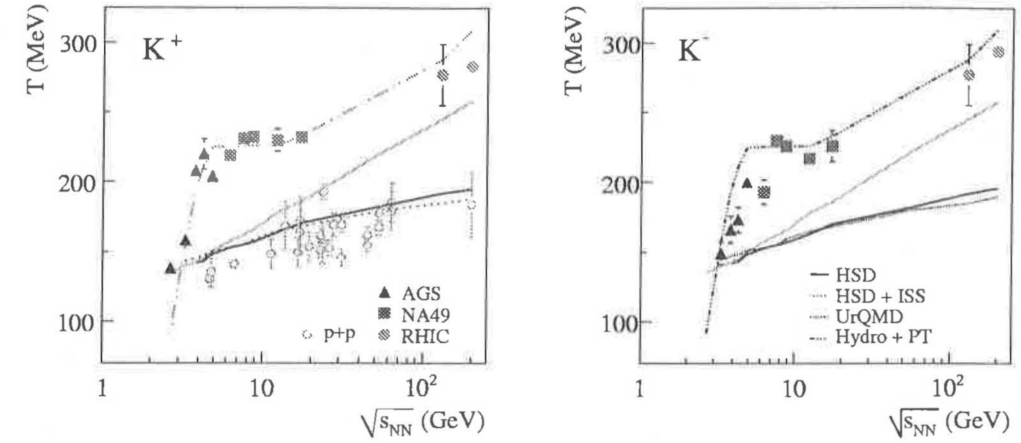

Figure 4: Energy dependence of the inverse slope parameter T of transverse mass spectra for K^+ (left) and K^- (right) [4]. The data are compared to results of UrQMD [16] and HSD [17] models, and hydrodynamical model (Hydro+PT) [18] incorporating the first order phase transition.

2.4 Verification of NA49 results by STAR and ALICE

Until now the evidence of the onset of deconfinement was based on the results of a single experiment. Recently new results on central Pb+Pb collisions at the LHC [24] and data on central Au+Au collisions from the RHIC BES (Beam Energy Scan) program [25] were released. Figure 5 (left) shows an update of the kink plot, where BES points follow the line for $A+A$ collisions and the LHC point [2], within a large error, does not contradict extrapolations from high SPS and RHIC energies.

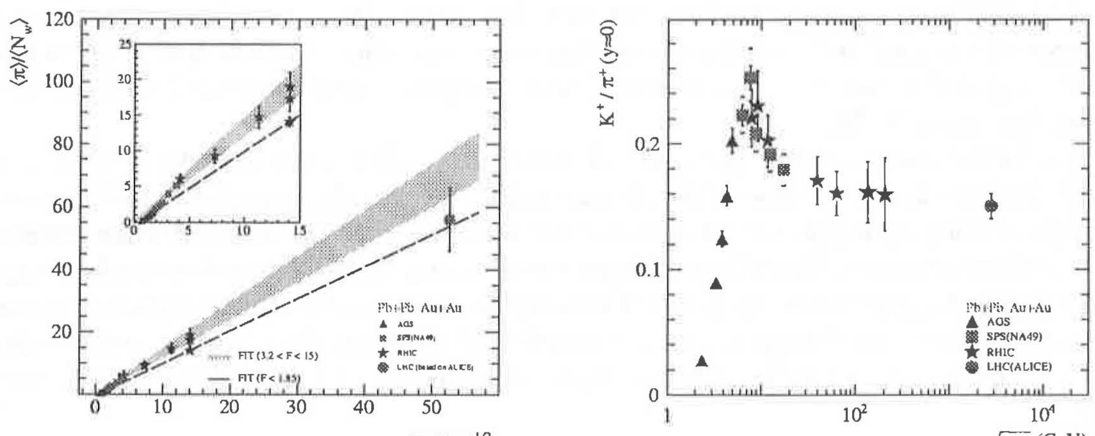

Figure 5: Mean pion multiplicity per participant nucleon (left). Kaon to pion yield near midrapidity (right). See [26] for details.

The K^+/π^+ yield (near midrapidity) is presented in Fig. 5 (right). Figure 6 shows inverse slope parameters of kaon transverse mass spectra. The LHC points and the RHIC BES points confirm the step structure expected for the onset of deconfinement. As seen, RHIC results confirm NA49 measurements at the onset of deconfinement. Moreover, LHC (ALICE) data demonstrate that the energy dependence of hadron production properties shows rapid changes

[2] the mean pion multiplicity at LHC was estimated based on the ALICE measurement of charged particle multiplicity, see [26] for details.

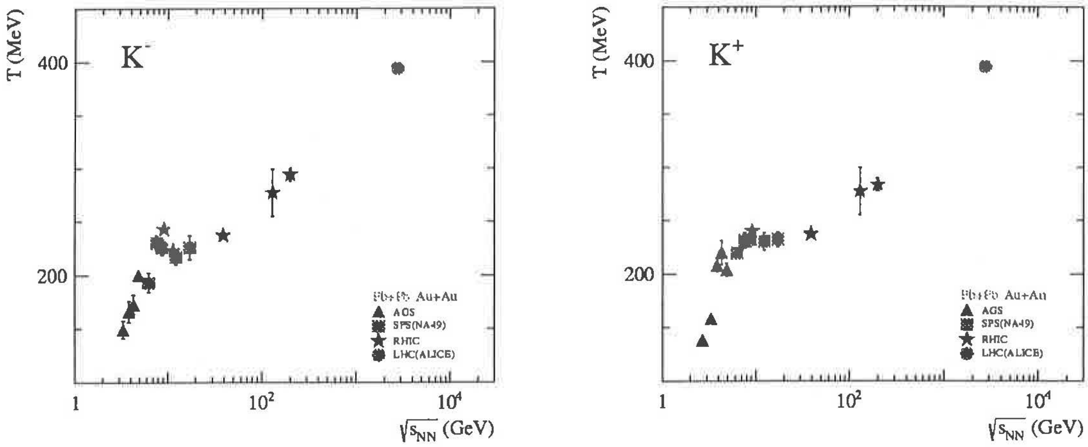

Figure 6: Inverse slope parameters of kaon transverse mass m_T spectra. See [26] for details.

only at low SPS energies, and a smooth evolution is observed between the top SPS (17.2 GeV) and the current LHC (2.76 TeV) energies. All three structures confirm that results agree with the interpretation of the NA49 structures as due to the onset of deconfinement. Above the onset energy only a smooth change of QGP properties with increasing energy is expected.

3 Critical point and phase transition in fluctuations

The QCD phase diagram [27] is often plotted in terms of tempeerature (T_{chem}) and baryochemical potential (μ_B). The lattice QCD calculations indicate that at small chemical potential ($\mu_B \approx 0$) the transition from hadronic to partonic matter is a crossover [28], while at larger values of μ_B the transition becomes first order [29]. Therefore, one expects the existence of a critical point at the end of first order transition. Several lattice QCD calculations suggest the existence of the critical point (CP) of strongly interacting matter in the SPS energy range [8, 30]

One of the characteristic signatures of the critical point is an increase in fluctuations of various event-by-event observables, in particular the particle multiplicity and transverse momentum fluctuatios [12, 13]. A signal of CP is expected to be maximal when freeze-out of the system created in the collision happens near critical point. These observations suggest that it might be possible to perform a 2-dimentional scan of the phase diagram of strongly interacting matter by changing $\sqrt{s_{NN}}$ (variation of μ_B) and the colliding system size A (variation of T_{chem}) and look for a maximum of fluctuations as a signature for the critical point.

3.1 Transverse momentum and multiplicity fluctuations

In NA49 the Φ_{p_T} measure [31, 32, 33] and the scaled variance ω [34, 35, 36] are used for studying the mean transverse momentum and particle multiplicity fluctuations, respectively.

The Φ_{p_t} measure is defined as

$$\Phi_{p_t} = \sqrt{\frac{\langle Z_{p_t}^2 \rangle}{\langle N \rangle}} - \sqrt{\overline{z_{p_t}^2}}, \tag{1}$$

where $z_{p_t} = p_t - \overline{p_t}$ with the bar denoting the overall inclusive average and $Z_{p_t} = \sum_{i=1}^{N}(p_{ti} - \overline{p_t})$ with summation over the event multiplicity N. Thus, the Φ_{p_t} represents the difference between the event average of a quantity $\langle p_t \rangle$ and its ensemble average expressed by the first and second terms of Eq.1, respectivelly.

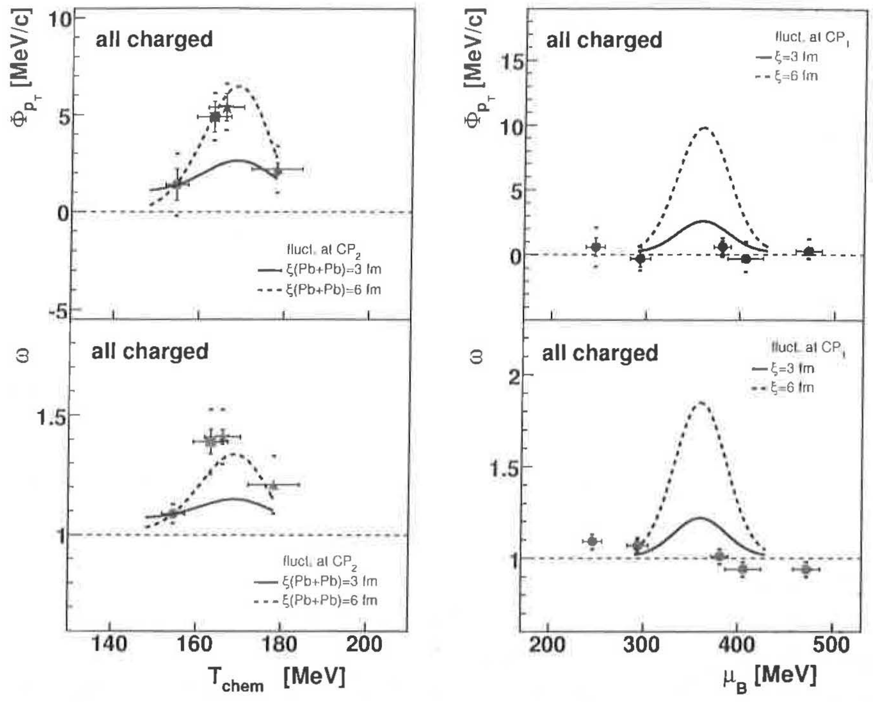

Figure 7: Fluctuation measures Φ_{p_t} of average transverse momentum and ω the scaled variance of the multiplicity distribution versus freeze-out temperature T (left) and baryochemical potential μ_B (right) measured by NA49. Dashed and solid lines indicate the estimated effects of the critical point for two values of the correlation lenght ξ (size of the fireball).

For multiplicity fluctuation the scaled variance ω (variance of the multiplicity distribution normalized by its mean value) is defined as

$$\omega = \frac{Var(n)}{\langle n\rangle} = \frac{\langle n^2\rangle - \langle n\rangle^2}{\langle n\rangle} \tag{2}$$

The results of the NA49 study of transverse momentum [33] and multiplicity [35, 36] fluctuations are plotted in Fig.7 [37, 38].

It presents the energy (μ_B) and system size (T_{chem}) dependence of Φ_{p_t} and ω. The chemical freeze-out parameters, $T_{chem}(A, \sqrt{s_{NN}})$ and $\mu_B(A, \sqrt{s_{NN}})$ were taken from fits of the hadron gas model [10] to particle yields. The lines correspond to predictions for critical points CP_1 and CP_2 with estimated magnitude of the effect for Φ_{p_t} and ω taken from [12, 39, 40], assuming correlation lenghts ξ decreases monotonicaly with decreasing system size (fireball), namely ξ(Pb+Pb) = 6 fm and ξ(p+p) = 2 fm (dashed lines) or ξ(Pb+Pb) = 3 fm and ξ(p+p) = 1 fm (solid lines).

As possible location of the critical point CP_1 (Fig.7 (right)) the μ_B = 360 MeV was taken from lattice QCD calculations [8] and the corresponding T_{chem} = 147 MeV to be on the empirical freeze-out line for the 5 energies of central Pb+Pb collisions. For critical point CP_2 (Fig.7 (left)) the measured chemical freeze-out parameters of p+p reaction at 158 GeV, μ_B = 250 MeV and T_{chem} = 178 MeV, were suggested assuming that this point may be located on the phase transition line.

Fig.7 (right) shows no significant energy dependence of mean p_t and multiplicity fluctuations at SPS energies. Thus the results do not provide evidence for for critical point CP_1 making possible conclusions that either the critical point is not close enough to manifest itself in the data or the correlation length realized in heavy ion collisions is very small.

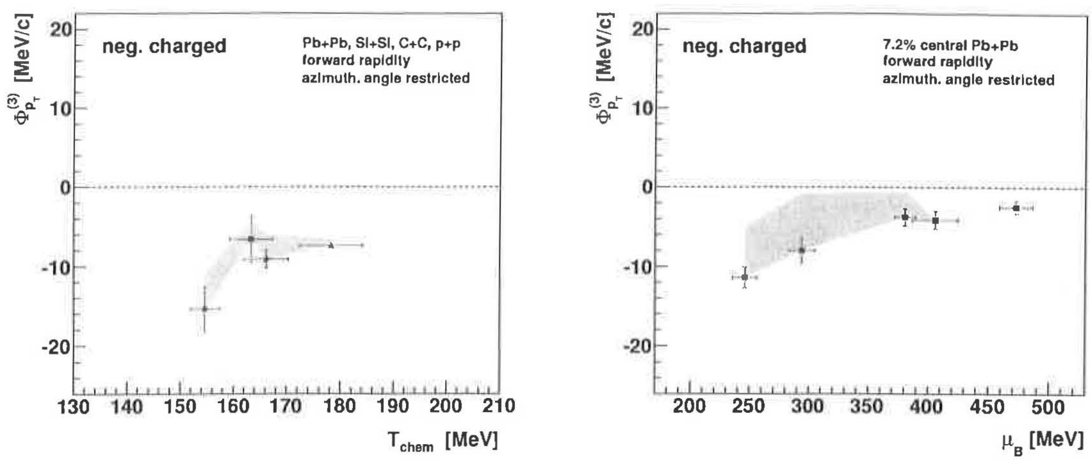

Figure 8: (NA49 very preliminary) Third moment $\Phi^{(3)}_{p_t}$ of average transverse momentum fluctuations versus T (left) and μ_B (right) for negatively charged particles.

The system size dependence of fluctuations presented in Fig.7 (left) exibits a maximum of Φ_{p_t} and ω for intermediate systems C+C and Si+Si interactions at the top SPS energy. The peak is two times higher for all charged than for negatively charged particles as expected for the critical point [12]. Both figures suggest that the NA49 data are consistent with the CP_2 predictions for possible critical point at $\mu_B \approx 250$ MeV and $T_{chem} \approx 165$ MeV.

3.2 Higher moments of transverse momentum fluctuations

Most fluctuation measures discussed to date can be related to a quadratic variances (second moments) of event-by-event observables, such as particle multiplicities, net charge, baryon number, particle ratios, or mean transvere momentum in the event.

For future fluctuation studies, the higher moments of event-by-event distribtions will be of great interest. It was ponted out [41, 42, 43] that the higher moments of fluctuations are much more sensitive to the proximity of the critical point than the commonly employed measures based on the quadratic measures. In this case the amplitude of the critical point peak became proportional to higher powers of the correlation length ξ.

The first attempt of NA49 in studying the higher moment fluctuations was applied to the mean p_t observable using the Φ measure. In general case, the n-th moment is defined as

$$\Phi^{(n)}_{p_t} = \left(\frac{\langle Z^n_{p_t}\rangle}{\langle N\rangle}\right)^{1/n} - \left(\overline{z^n_{p_t}}\right)^{1/n} \qquad (3)$$

In present analysis, the third moment $\Phi^{(3)}_{p_t}$ was employed. A very preliminary results on the system size (T) and the energy (μ_B) dependences of the $\Phi^{(3)}_{p_t}$ are presented in Fig.8 (left) and Fig.8 (right), respectively. Some dependence of the $\Phi^{(3)}_{p_t}$ on the mentioned parameters is visible but no evident maximum is observed. For further study of higher moment fluctuations the progress in data analysis and the relevant theoretical predictions are necessary.

3.3 Density fluctuations of low-mass $\pi^+\pi^-$ pairs and protons

At the critical point (CP) local density fluctuations with the power-law singularity are expected both in configuration and momentum space [44] and should appear both for baryonic density and the σ field. It is motivated by the hypothesis that magnitude the net-baryon density and σ field characterise the order parameters for the second order phase transition associated with the QCD critical endpoint.

Significant σ-field fluctuations are expected at the CP (density fluctuations of zero mass σ-particles produced in abundance at the CP) [44]. σ particles at $T < T_c$ may reach the two-pion threshold ($2m_\pi$) and then decay into two pions, therefore density fluctuations of di-pions with $m_{\pi^+\pi^-}$ close to the two pion mass incorporate σ–field fluctuations at the CP.

Critical σ fluctuations are predicted to be observable as an intermittency behaviour of the second order factorial moments [45]. The NA49 experiment searched for an intermittency signal in transverse momentum space of reconstructed di-pions ($\pi^+\pi^-$ pairs) with invariant mass just above $2m_\pi$ [46]. The analysis was performed for p+p, C+C and Si+Si interactions at 158A GeV. First, for each event all possible pairs with $m_{\pi^+\pi^-}$ in a small kinematic window above two-pion threshold were selected. Then, second factorial moments $F_2(M)$ in transverse momentum space were computed for real data and for artificially produced mixed events where only statistical fluctuations are present. The second factorial moment of the di-pion density

$$F_2(M) = \langle \frac{1}{M^2} \sum_{i=1}^{M^2} n_i(n_i - 1) \rangle / \langle \frac{1}{M^2} \sum_{i=1}^{M^2} n_i \rangle^2 \qquad (4)$$

was calculated as a function of the number M of subdivisions in each transverse momentum space direction (-1.5 GeV/$c < p_{T,x}, p_{T,y} < 1.5$ GeV/c), where n_i is the number of di-pions in the cell i. The combinatorial background subtracted (by use of mixed events) moments ΔF_2 in transverse momentum space are expected to follow a power-law behavior $\Delta F_2 \sim (M^2)^{\phi_2}$, with $\phi_{2,cr} = 2/3$ for system of a low-mass $\pi^+\pi^-$ pairs freezing out at the QCD critical point [44].

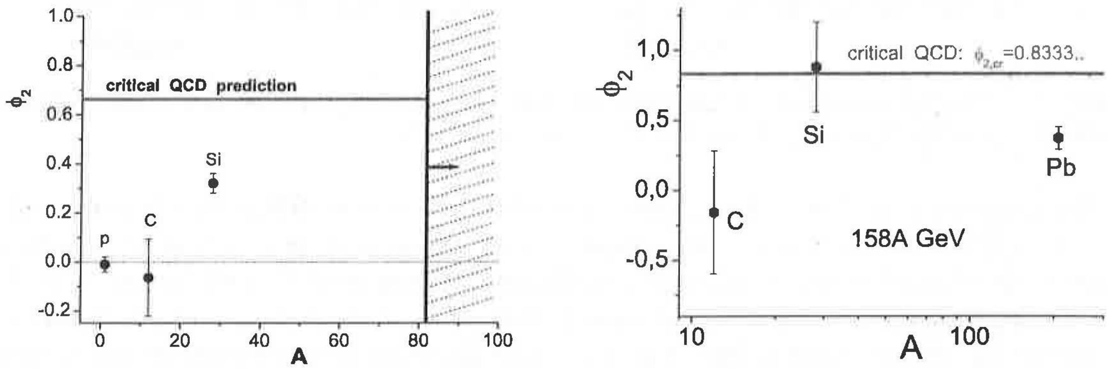

Figure 9: Intermittency signal in p+p and 10% most central C+C and Si+Si interactions at 158A GeV [46] presented in the dependence of intermittency index ϕ_2 on the size A of the colliding nuclei for a systems of low-mass $\pi^+\pi^-$ pairs (left) and net protons (right). The upper horizontal lines indicate the theoretical expected values $\phi_{2,cr} = 2/3$ and $\phi_{2,cr} = 5/6$ for a low-mass $\pi^+\pi^-$ pairs and net protons respectively, freezing out at the QCD critical point.

There is a clear intermittency signal observed in the data although somewhat weaker than in simulation of critical behaviour. Figure 9 (left) shows that ΔF_2 for Si+Si at the top SPS energy measures fluctuations approaching in size the prediction of critical QCD (the remaining departure, $\phi_{2,max} \approx 0.33 \pm 0.04$ instead of 2/3, may be due to freezing out at a distance from the CP). As expected, the analysis of Si+Si events generated via the HIJING model shows no intermittency signal ($\phi_2 \approx 0.02 \pm 0.09$).

From the results of preliminary analysis, a strong intermittency signal is also found in transverse momentum space of protons Fig.9 (right) for Si cluster right compatible with above fluctuation results in the di-pion sector. These findings support further the view that the central Si+Si collision system leads to freeze-out state in the neighbourhood of the QCD critical point.

3.4 Azimuthal angle fluctuations

The main motivation of studying azimuthal event-by-event fluctuations was to search for plasma instabilities [47], critical point and onset of deconfinement, and flow fluctuations [48]. NA49 evaluated the Φ measure of fluctuations (instead of using p_T, as in section 3.1, one uses azimuthal angle ϕ). There are several background effects that can influence the Φ_ϕ measure, among them resonance decays, flow, (di-)jets, momentum conservation, quantum statistics. All of them were studied in [49].

Figure 10 shows the energy dependence of Φ_ϕ for the 7.2% most central Pb+Pb interactions. Color bands represent systematic errors. The values for positive particles are consistent with zero but for negative particles Φ_ϕ is positive. No collision energy dependence of the fluctuations is observed.

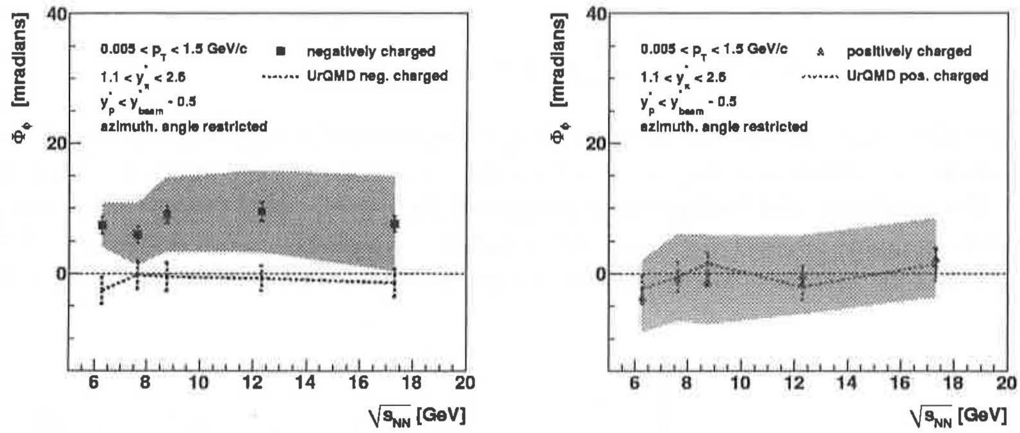

Figure 10: Energy dependence of azimuthal fluctuations. Forward rapidity, limited azimuthal acceptance (as in [50]). The same acceptance for data and UrQMD.

The system size and centrality dependence of Φ_ϕ at the top SPS energy is presented in Fig. 11. For Pb+Pb collisions, the sample of events was split into six centrality classes. Figure 11 shows positive Φ_ϕ values with a maximum for peripheral Pb+Pb interactions. The data are not explained by the UrQMD model. However, the magnitude of Φ_ϕ is reproduced by the effect of directed and elliptic flow [52]. The difference between positive and negative particles is also reproduced and it is caused by a 15% admixture of protons among positive particles (in the MC model calculation [52] v_1 and v_2 values for pions and protons at forward rapidity were taken from [53]).

3.5 Particle ratio fluctuations

In addition to the hadron production properties observed at the phase transition several models suggest the study of hadron ratio fluctuations to gain further insight into the nature of the deconfinement phase transition. Particle ratio fluctuations might also be affected by the critical point.

The measurement of hadron ratio fluctuations by NA49 is expressed in terms of dynamical fluctuations σ_{dyn} which referes to those fluctuations remaining after removing fluctuations

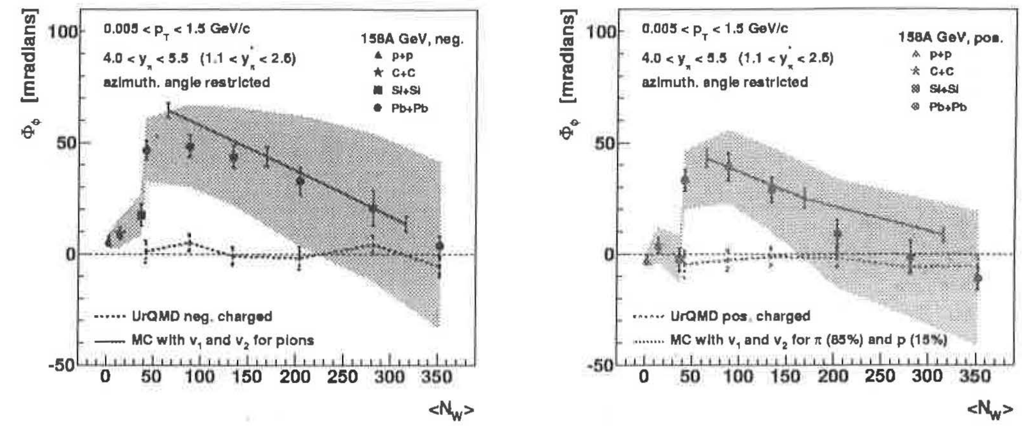

Figure 11: System size dependence of azimuthal fluctuations. Forward rapidity, limited azimuthal acceptance (as in [51]). The same acceptance for data and UrQMD.

from finit number statistics as well as effects from detector resolution and particle identification. The dynamical fluctuation is defined as

$$\sigma_{dyn} = sign(\sigma^2_{data} - \sigma^2_{mix})\sqrt{| \sigma^2_{data} - \sigma^2_{mix} |}. \tag{5}$$

It measures the difference between widths of the particle ratio distributions for data σ_{data} and for artificially produced mixed events σ_{mix} , where only statistical fluctuations are present (see [54] for details). .

The energy dependence of event-by-event fluctuations of the particle ratios K/π and p/π (for the 3.5% most central Pb+Pb collisions) is shown in Fig. 12. K/π fluctuations show positive values of σ_{dyn}. The steep rise towards low SPS energies is not reproduced by the UrQMD model. The HSD model catches the trend but over-predicts high energy SPS results. The p/π ratio shows negative dynamical fluctuations. This behavior is reproduced by hadronic models and understood in terms of correlations due to nucleon resonance decays.

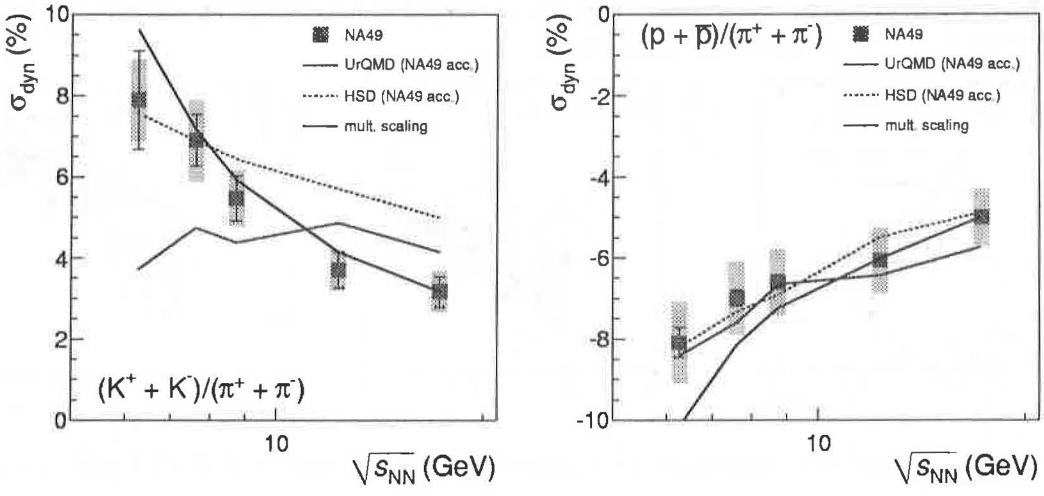

Figure 12: Energy dependence of K/π and p/π fluctuations [54].

An unexpected result was obtained for event-by-event K/p fluctuations (Fig. 13). Dynamical fluctuations change sign close to the onset of deconfinement energy. A jump to positive values at lowest SPS energies is followed by a negative plateau at higher SPS energies. Such structure is not described by hadronic models (UrQMD and HSD). Additionally we show K^+/p fluctuations in which no contributions from resonance production are expected. The relation of this intriguing result to the onset of deconfinement is not known yet.

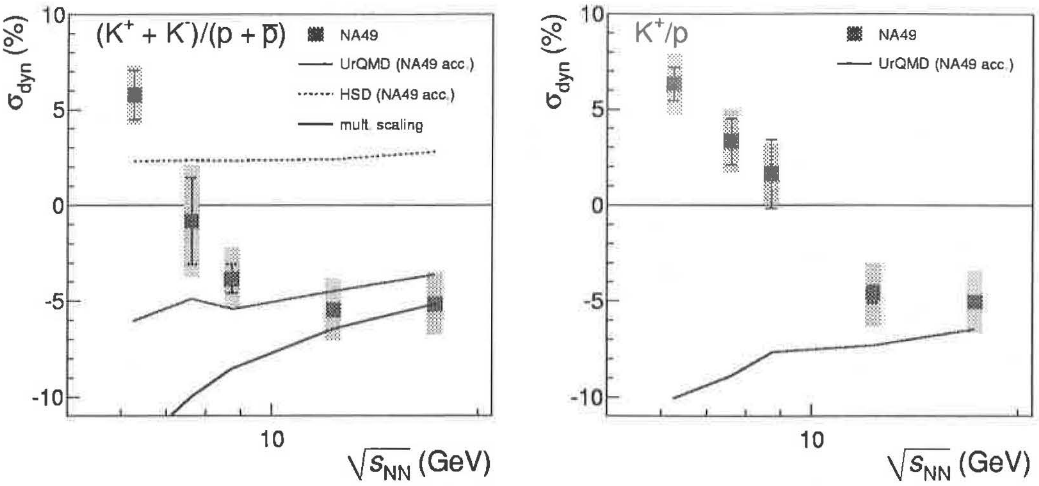

Figure 13: Energy dependence of K/p fluctuations [54].

It has been suggested [55] that σ_{dyn} can be separated into two terms: a correlation strength term and a term purely dependent on multiplicities. In case of unchanged correlations (invariant correlation strength) the general expectation is $\sigma_{dyn} \propto \sqrt{\frac{1}{\langle A \rangle} + \frac{1}{\langle B \rangle}}$, where $A, B = N_K, N_\pi, N_p$, etc. Such scaling is presented in Figs. 12, 13 as black solid lines. One can see that scaling works very well for K/π and p/π fluctuations. The change of sign in K/p fluctuations excludes any simple scaling based on average multiplicities. The above scaling assumed invariant correlation strength, therefore the NA49 results suggest that the underlying correlation between kaons and protons is changing with energy.

The centrality dependence of event-by-event particle ratio fluctuations at 158A GeV ($\sqrt{s_{NN}}$ = 17.3 GeV) is presented in Fig. 14. The absolute values of fluctuations rise towards peripheral collisions, as in UrQMD. The same multiplicity scaling (as in Figs. 12, 13) seems to hold for all three particle ratio fluctuations (black, solid lines in Fig. 14). This is compatible with the hypothesis that at constant energy the underlying correlations are not significantly changing with the system size.

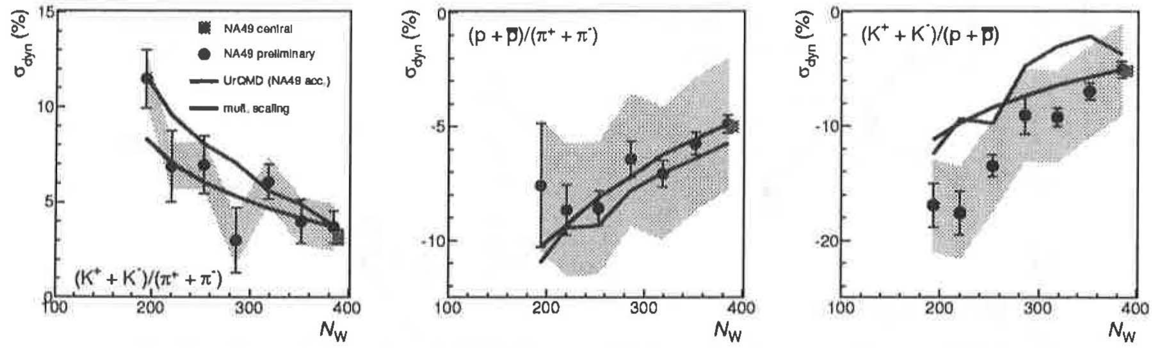

Figure 14: Centrality dependence of particle ratio fluctuations at 158A GeV [54].

4 Research program of NA61/SHINE experiment

The NA61/SHINE experiment at the CERN SPS [56] will continue the program of NA49 with the main goal of searching for the QCD critical point and studying in details the onset of deconfinement by performing a two-dimensional scan (T versus μ_B) of the phase diagram (Fig.1). This will be achieved by varying collision energy (13A - 158A GeV) and size of the

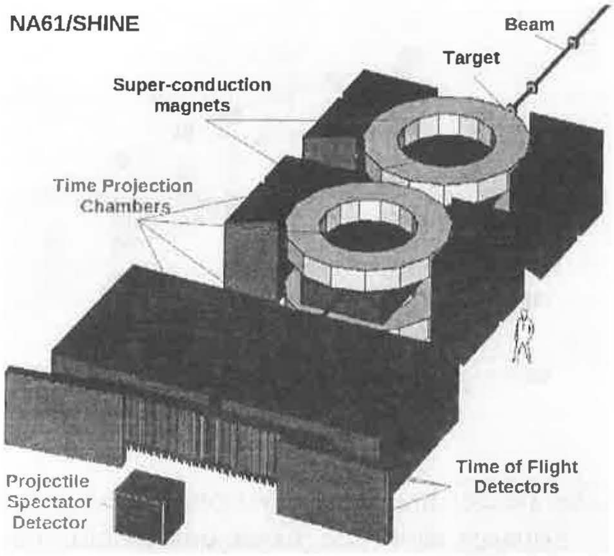

Figure 15: Layout of experiment NA61/SHINE at the CERN SPS.

colliding systems (p+p, p+Pb, B+C, Ar+Ca, Xe+La) in order to cover a broad range of the phase diagram of hadronic matter.

The NA61 experiment (Fig.15) is the successor of NA49. Several upgrades of the detector apparatus inherited from NA49 are complited or in progess.

The first part of the system size and energy scan program, namely p+p collisions at 13, 20, 30, 40, 80 and 158 GeV/c beam energies is being performed [57]. High statistics data on p+p has already been recorded in 2009 and 2010, and will be recorded in 2011. The ion B+C, Ar+Ca and Xe+La runs are foreseen for 2011, 2013 and 2014, respectivelly. They will allow to cover a broad range of parameters T and μ_B of the phase diagram. These parameters vary under changes of the system size and collision energy. The hypothetical positions of the chemical freeze-out points expected for central nucleus-nucleus collisions are shown in Fig.16.

The NA61 program will be complemented by the efforts of other laboratories, BNL RHIC ($5 < \sqrt{s_{NN}} < 39$ GeV), JINR NICA ($3 < \sqrt{s_{NN}} < 9$ GeV), GSI SIS-100(300) ($2.3 < \sqrt{s_{NN}} <$ 8.5 GeV).

5 Summary and conclusions

Experiments of NA49 at CERN SPS motivated by predictions of the Statistical Model of the Early Stage indicate that deconfinement starts to occure at the early stage of central Pb+Pb collisions for beam energies above $\sim 30A$ GeV.

The NA49 discovery of the energy threshold for deconfinement is now confirmed. The results from the RHIC Beam Energy Scan agree with NA49 measurements on the onset of deconfinement. LHC data confirm the interpretation of the structures observed at low SPS energies as due to onset of deconfinement.

The NA49 also searched for indications of the predicted QCD critical point where an enhanced event-by-event multiplicity and mean transverse momentum fluctuations are expected. The results from energy scan (variation of baryonic chemical potencial μ_B) in central Pb+Pb collisions show no evidence for the expected critical point location at $\mu_B \approx 360$ MeV and $T_{chem} \approx 150$ MeV, while a visible fluctuations are seen in system size dependence (variation of temperature T_{chem}) for relatively lighter systems produced in $158A$ GeV C+C and Si+Si collisions at $\mu_B \approx 250$ MeV and $T_{chem} \approx 165$ MeV.

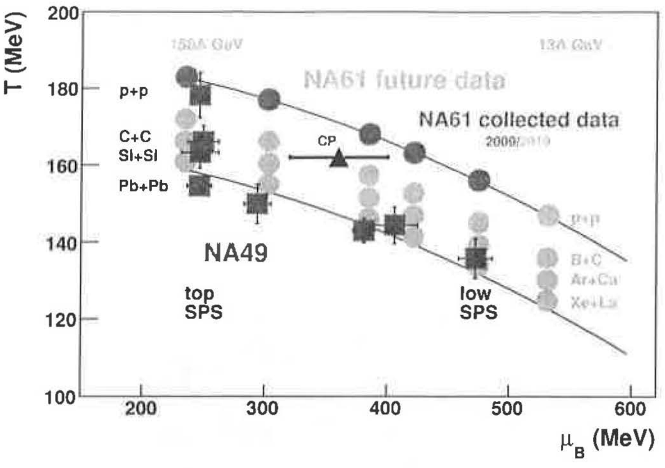

Figure 16: Scan of the phase diagram by varying collision energy (μ_B) and size of colliding nuclei (T). Squares show the freeze-out points covered by NA49, circles indicate the planned measurements of NA61. The estimated location of the critical point is shown be the triangle.

Analysis of density fluctuations of low-mass di-pions (sigma sector) for central Si+Si collisions shows a clear intermittency signal. Compatible fluctuation results is also found from preliminary analysis in transvere momentum of protons. These findings support further the view that the central Si+Si collision system may lead to freeze-out state in the neighbourhood of the QCD critical point.

The azimuthal angle fluctuatuations of charged particles were analyzed using the Φ_ϕ measure. The measurements for central Pb+Pb collisions shows weak energy dependence of Φ_ϕ. However, in the system size dependence the significant rise of the measured fluctuations towards a smaller colliding systems are indicated. This is qualitatively similar to the mean transverse momentum and multiplicity fluctuation results obtained in NA49.

The energy and the system size dependence of K/π and p/π fluctuations can be described in a simple multiplicity scaling model. In contrast, K/p fluctuations show a deviation from this scaling and change sign close to the onset of deconfinement energy; is the underlying correlation physics changing with energy?

For central $A + A$ collisions fluctuations of average p_T, multiplicity, and multiplicity of low mass $\pi^+\pi^-$ pairs and net protons tend to a maximum in Si+Si collisions at 158A GeV. Thus the critical point may be accessible at SPS energies. This result is a strong motivation for future experiments and in fact, the NA49 efforts will be continued by the ion program of the NA61/SHINE experiment .

A further detailed energy and system size scan to investigate the properties of the onset of deconfinement and to establish the existence of the QCD critical point is being performed in the NA61/SHINE experiment at the CERN SPS in order to cover a broad range of the phase diagram of strongly interacting matter.

References

[1] T. Alber *et al.* (NA49 Collaboration), Phys. Rev. Lett. **75** (1995) 3814.

[2] U .W. Heinz and M. Jacob, arXiv:nucl-th/0002042.

[3] M. Gaździcki and M .I .Gorenstein, Acta Phys. Polon. B**30** (1999) 2705.

[4] C. Alt *et al.* (NA49 Collaboration), Phys. Rev. C **77** (2008) 024903.

[5] M. Gaździcki, J.Phys. **G30** (2004) S701.

[6] P. Seyboth, Acta Phys. Polon. B**37** (2006) 3429.

[7] V. Friese (NA49 Collaboration), PoS **CPOD09** (2009) 005.

[8] Z. Fodor and S .Katz, J. High Energy Phys.**0404** (2004) 050.

[9] P. Braun-Munzinger, J. Cleymans, H. Oeschler and K. Redlich, Nucl. Phys. **A697** (2002) 902.

[10] F. Becattini, J. Manninen and M. Gaździcki , Phys. Rev. C **73** (2006) 044905.

[11] F. Becattini, M. Gaździcki, A. Keranen amd R. Stock, Phys. Rev. C **69** (2004) 024905.

[12] M. A. Stepanov, K. Rajagopal and E. V. Shuryak, Phys. Rev. D **60** (1999) 114028.

[13] V. Koch, arXiv:0810.2520 [nucl-th].

[14] S. Afanasiev *et al.* (NA49 Collaboration), Nucl. Instrum. Methods. A **430** (1999) 210.

[15] H. Sorge, H. Stocker and W. Greiner, Nucl. Phys. **A498** (1989) 567.

[16] S. A. Bass *et al.*, Prog. Part. Nucl. Phys. **41** (1998) 225.

[17] E. I. Bratkovskaya *et al.*, Phys. Rev. C **69** (2004) 054907.

[18] M. Gaździcki,M. I. Gorenstein, F. Grassi, Y. Hama, T. Kodama, and O. J. Sokolowski, Braz. J. Phys. **34** (2004) 322.

[19] H. Petersen and M. Bleicher, PoS **CPOD2006** (2006) 025.

[20] S. Akkelin and Y. Sinyukov Phys. Rev. C **73** (2006) 034908.

[21] L. Kumar *et al.* (STAR Collaboration), J. Phys. G **36** (2009) 064066.

[22] G. Wang *et al.* (STAR Collaboration), Nucl. Phys. **A830** (2009) 19c.

[23] D. Cebra *et al.* (STAR Collaboration), arXiv: 0903.4702 [nucl-ex].

[24] J. Schukraft (for ALICE Collab.), *J. Phys.* **G38**, 124003 (2011);
A. Toia (for ALICE Collab.), *J. Phys.* **G38**, 124007 (2011).

[25] L. Kumar (for STAR Collab.), *J. Phys.* **G38**, 124145 (2011);
B. Mohanty (for STAR Collab.), *J. Phys.* **G38**, 124023 (2011).

[26] A. Rustamov, https://indico.cern.ch/conferenceDisplay.py?confId=144745

[27] K. Rajagopal and F. Wilczek, arXiv:hep-ph/0011333.

[28] C. Bernard *et al.*, Phys. Rev. D **75** (2007) 094905.

[29] O. Scavenius *et al.*, Phys. Rev. C **64** (2001) 045202.

[30] P. Gavai and S. Gupta, Phys. Rev. D **78** (2008) 114503.

[31] M. Gaździcki and St. Mrówczyński, Z.Phys. C **54** (1992) 127.

[32] T. Anticic *et al.* (NA49 Collaboration), Phys. Rev. C **70** (2004) 034902.

[33] T. Anticic *et al.* (NA49 Collaboration), Phys. Rev. C **79** (2009) 044904.

[34] C. Alt *et al.* (NA49 Collaboration), Phys. Rev. C **75** (2007).064904.

[35] C. Alt *et al.* (NA49 Collaboration), Phys. Rev. C **78** (2008) 034914.

[36] B. Lungwitz, PhD thesis (2008), http://edms.cern.ch/document/989055/1.

[37] K. Grebieszkow *et al.* (NA49 Collaboration), arXiv:0907.4101 [nucl-ex].

[38] K. Grebieszkow *et al.* (NA49 and NA61 Collaboration), arXiv:0909.0485 [hep-ex].

[39] M. Stepanov, private communications.

[40] Y. Hatta and T. Ikeda, Phys. Rev. D **67** (2003) 014028.

[41] St. Mrówczyński, Phys. Lett. **B465** (1999) 8.

[42] M. A. Stepanov, Phys. Rev. Lett. **102** (2009) 032301.

[43] M. Cheng *et al.*, Phys. Rev. D **79** (2009) 074505.

[44] N. Antoniou *et al.* (NA49 collaboration), Nucl. Phys. **A761** (2005) 149.

[45] A. Bialas and R. Peschanski, Nucl. Phys. **B273** (1986) 703.

[46] T. Anticic *et al.* (NA49 Collaboration), Phys. Rev. C **81** (2010) 064907.

[47] St. Mrówczyński, *Phys. Lett.* **B314**, 118-121 (1993).

[48] St. Mrówczyński and E. V. Shuryak, *Acta Phys. Polon.* **B34**, 4241 (2003).

[49] St. Mrówczyński, *Acta Phys. Polon.* **B31**, 2065 (2000);
T. Cetner, K. Grebieszkow, St. Mrówczyński, *Phys. Rev.* **C83**, 024905 (2011).

[50] T. Anticic et al. (NA49 Collab.), *Phys. Rev.* **C79**, 044904 (2009).

[51] T. Anticic et al. (NA49 Collab.), *Phys. Rev.* **C70**, 034902 (2004).

[52] K. Grebieszkow and St. Mrówczyński, arXiv:1110.4910

[53] C. Alt et al. (NA49 Collab.), *Phys. Rev.* **C68**, 034903 (2003).

[54] T. Schuster (for NA49 Collab.), *J. Phys.* **G38**, 124096 (2011) and ref. therein.

[55] V. Koch and T. Schuster, *Phys. Rev.* **C81**, 034910 (2010).

[56] N. Antoniou *et al.* (NA61 Collaboration), Proposal CERN-SPSC-2006-034/P-330 and addenda.

[57] M. Gaździcki (for NA49 and NA61 Collab.), *J. Phys.* **G38**, 124024 (2011).